UCRL-JRNL-232518

LAWRENCE
LIVERMORE
NATIONAL
LABORATORY

Single molecule study of a processivity clamp sliding on DNA

T. A. Laurence, Y. Kwon, A. Johnson, C. Hollars, M. O'Donnell, J. A. Camarero, D. Barsky

July 5, 2007

Journal of Biological Chemistry

Single molecule study of a processivity clamp sliding on DNA

Ted A. Laurence[A,C], Youngeun Kwon[A], Aaron Johnson[B], Chris Hollars[A], Mike

O'Donnell[B], Julio A. Camarero[A], and Daniel Barsky[A,C]

[A]Chemistry, Materials, and Life Sciences, Lawrence Livermore National Laboratory,

California, USA 94550

[B]Rockefeller Univ and Howard Hughes Med Inst, New York, NY, USA

Summary

Using solution based single molecule spectroscopy, we study the motion of the polIII β-

subunit DNA sliding clamp ("β-clamp") on DNA. Present in all cellular (and some

viral) forms of life, DNA sliding clamps attach to polymerases and allow rapid,

processive replication of DNA. In the absence of other proteins, the DNA sliding clamps

are thought to "freely slide" along the DNA; however, the abundance of positively

charged residues along the inner surface may create favorable electrostatic contact with

the highly negatively charged DNA. We have performed single-molecule measurements

on a fluorescently labeled β-clamp loaded onto freely diffusing plasmids annealed with

fluorescently labeled primers of up to 90 bases. We find that the diffusion constant for

1D diffusion of the β-clamp on DNA satisfies $D \leq 10^{-14}$ $\mathrm{cm^2/s}$, much slower than the

frictionless limit of $D = 10^{-10}$ $\mathrm{cm^2/s}$. We find that the β clamp remains at the 3' end in

the presence of *E. coli* single-stranded binding protein (SSB), which would allow for a

sliding clamp to wait for binding of the DNA polymerase. Replacement of SSB with

Human RP-A eliminates this interaction; free movement of sliding clamp and poor

binding of clamp loader to the junction allows sliding clamp to accumulate on DNA.

This result implies that the clamp not only acts as a tether, but also a placeholder.

[C] To whom correspondence should be addressed: T. A. L. (laurence2@llnl.gov) and D. B.

(daniel_barsky@cornell.edu)

Introduction

DNA sliding clamp proteins increase enzymatic processivity of DNA polymerases

during DNA synthesis. Without them, replication of long stretches of DNA would be

infeasible because DNA polymerases tend to fall off the DNA after elongating a strand

by only a few bases. By tethering the polymerase to the DNA, such processivity factors

enable the polymerase to add up to a thousand bases per second without detaching from

the DNA (Fay et al., 1981; O'Donnell and Kornberg, 1985). The term "sliding clamp"

aptly described a protein that tethers the polymerase to the DNA, and yet can still travel

vast distances along the DNA. The remarkable ring-shaped structure of the major

prokaryotic and eukaryotic DNA sliding clamps (Kong et al., 1992; Gulbis et al., 1996)

provides a beautifully simple mechanism for sliding without falling off: the proteins form

a closed ring around DNA and slide along like a washer—or possibly a nut—on a very

long bolt.

The major clamps associated with DNA replication are the dimeric polymerase III, β

subunit (or β clamp) in prokaryotes and the trimeric Proliferating Cell Nuclear Antigen

(PCNA) clamp in eukaryotes and archaea. In addition to their important role in DNA replication processivity, DNA sliding clamps have been found to be involved in a large number of processes dealing with DNA metabolism (Maga and Hubscher, 2003; Vivona and Kelman, 2003; Majka and Burgers, 2004; Johnson and O'Donnell, 2005).   Seen to interact with a wide variety of proteins and protein complexes, they have been described as molecular tool-belts and moving platforms (Lopez de Saro and O'Donnell, 2001; Indiani et al., 2005).

   After being loaded onto DNA by a clamp loader complex, DNA sliding clamps are stably attached to the DNA (Yao et al., 1996), yet move with the polymerase. In the absence of a polymerase, the DNA sliding clamps move along DNA by random thermal motion (one-dimensional diffusion). In experiments where the β clamp was loaded onto a nicked, circular 7200 base pair DNA plasmid, the β clamp was seen to remain on the circular plasmid with a half-life of an hour—three times the time of bacterial cell division (Yao et al., 1996). When the plasmid was linearized by a site-specific endonuclease, the β clamp was observed to disassociate within a few minutes, apparently by sliding off a free end of the DNA (Yao et al., 2000).

   The term "sliding" is ambiguous in the discussion above. The rate of one dimensional diffusion along DNA is critical to the behavior of the sliding clamp, and can provide insight into how DNA replication and repair is coordinated. The root mean square distance $\langle \Delta x^2 \rangle$ that the clamp diffuses depends on the time Δt by the relation $\langle \Delta x^2 \rangle = 2D\Delta t$, where D is the one dimensional diffusion constant. Consider the minimum time it takes a DNA polymerase attached to a sliding clamp to incorporate one

base, $\Delta t = 1$ ms. How far can the sliding clamp diffuse during that time? At one extreme, one can assume that the diffusion rate of the sliding clamp on DNA is limited only by the viscosity of water. Based on the size of the β clamp, the Stokes-Einstein relation provides an estimate of $D=5\times10^{-11}$ m²/s. For this diffusion rate, for $\Delta t = 1$ ms, the sliding clamp will have diffused an average distance of 300 nm ($x_m = \sqrt{\langle \Delta x^2 \rangle}$), or nearly 1000 bases. In this diffusion regime, it is critically important for proteins bound to the sliding clamp to remain consistently attached to the DNA, so that diffusion does not cause the protein complex to lose its place.

For very slow diffusion, the DNA polymerase would actively pull the sliding clamp along during polymerization. In the extreme case, all of the energy released in ATP hydrolysis during replication is needed to pull the sliding clamp at a constant velocity. Hydrolysis of 1 ATP to AMP in the extension of the DNA strand by one base provides about 8×10^{-20} J of energy in physiological conditions (Stryer, 1995). If all of this energy is used to pull against a constant drag force from the sliding clamp a distance of one base pair, the drag force is $F_{drag} \approx 200$ pN . The drag force is related to the velocity v according to $F_{drag} = \gamma v$, where the diffusion constant $D = kT/\gamma$. For a velocity v of 1000 base pairs per second, this gives $D \approx 1\times10^{-17}$ m^2/s .

The slide-off experiments described above can yield a crude lower limit on D. The linearization and gel filtration steps took approximately 15 minutes to complete, after which little or none of the sliding clamps were present on the linearized DNA. With this time, and assuming the average distance needed to diffuse was 3600 bases (half of the plasmid length), $D \geq 10^{-15}$ m^2/s. This already excludes the slowest diffusion cases, but

what is the true diffusion constant? In support of water limited diffusion along DNA is the observation that DNA sliding clamps have a large, overall negative charge. Such negative charge might create electrostatic repulsion and therefore free diffusive motion. However, there is a prevalence of positively charged (basic) residues on the inner surface capable of forming attractive salt bridges with DNA. Those favorable interactions would suggest energetic barriers to the clamp sliding along DNA that would slow down the diffusion along DNA.

   Even for relatively slow diffusion, near the lower limit found by the slide-off experiments, diffusion of the sliding clamp may cause mechanistic problems. For example, there is likely a time delay between when the clamp loader ejects the sliding clamp and when the DNA polymerase binds. For $D = 10^{-15} \, m^2/s$, a delay of 10 ms would allow the sliding clamp to diffuse an average distance of 12 base pairs, approximately the footprint of the sliding clamp on DNA. In order to prevent escape, the sliding clamp may either bind to the dsDNA-ssDNA junction, or accessory proteins at the junction such as SSB. Recent sliding clamp-DNA crystal structure indeed indicates the possibility of a direct interaction between the dsDNA-ssDNA junction and the sliding clamp (Roxana et al., submitted).   Interactions keeping the sliding clamp in place are likely especially important in lagging strand synthesis, since replication at each Okazaki fragment must be started anew, with an additional clamp loading and polymerase binding event. Also, pol I must complete the Okazaki fragments and remove RNA primers. Retention of the sliding clamp at this junction may allow efficient completion of this task. Binding to accessory proteins at the dsDNA-ssDNA junction would provide a simple,

elegant way for the sliding clamp to remain at the 3' end, waiting for the polymerase to bind.

To investigate these issues, we have measured the position and diffusion of the β clamp on DNA by single molecule fluorescence using alternating laser excitation (ALEX) (Kapanidis et al., 2004). ALEX has been successfully used to study DNA-protein interactions of RNA polymerase (Kapanidis et al., 2005; Kapanidis et al., 2006), and single molecule measurements have been used to study clamp loading pathways in the formations of the T4 bacteriophage DNA polymerase holoenzyme (Smiley et al., 2006). We obtain limits on rate of diffusion of the β clamp along DNA. We show that the β clamp diffuses slowly on DNA, with a diffusion constant of $D \leq 10^{-14}$ m^2/s, at least three orders of magnitude slower than free diffusion ($D=5\times10^{-11}$ m^2/s). We also find that the sliding clamp binds to the single-stranded binding protein (SSB) at the 3' end, which would allow for a sliding clamp to wait for binding of the DNA polymerase. Replacement of *E. coli* SSB with Human RP-A eliminates this interaction; free movement of sliding clamp and poor binding of clamp loader to the junction allows sliding clamp to accumulate on DNA. These results provide insight into how the sliding clamp remains in place during cycling of the polymerases during lagging strand synthesis. The fact that β clamp diffuses orders of magnitude more slowly on DNA than in water limited diffusion indicates the importance of staying in place even on shorter time scales. The slow diffusion may allow for swapping between different polymerase and the clamp loader/unloader without the clamp diffusing away.

Results

Single-molecule fluorescence resonance energy transfer (FRET) measurements allow the observation of dynamic, unsynchronized movement of the sliding clamp on the DNA (Fig. 1). We have used solution based single molecule methods to maximize the number of molecular complexes observed and to eliminate effects of immobilization schemes.

FRET is the distance dependent, non-radiative transfer of excitations from a donor fluorophore (D) to an acceptor fluorophore (A). The fraction of D excitations that transfer to A is called the FRET efficiency E. E depends on the distance R between D and A according to $E = 1 \big/ \left(1 + \left(R/R_0\right)^6\right)$, where R_0 (~5 nm) is the distance at which $E = 0.5$. We have used FRET to measure the distances between a β clamp fluorescently labeled with D and the 5' end of a section of dsDNA fluorescently labeled with A (Fig. 1A inset).

Two types of diffusion affect our experiments. First, there is 3D diffusion of fluorescently labeled molecules through the optical detection volume detected as photon bursts. Photon bursts are groups of photons (typically 50-500) that arrive at intense rates above the background level. In Figs. 1A and 1B, we illustrate the diffusion through the optical detection volume of the "β clamp-DNA complex," formed by loading fluorescently-labeled β clamp onto a fluorescently labeled DNA plasmid. Other fluorescently labeled species, including free β clamp and free DNA plasmids, diffuse through the detection volume as well. The time it takes for a β clamp-DNA complex to diffuse out of the detection volume (Fig. 1B) is dominated by the diffusion of the large plasmid. This "plasmid diffusion time" of 3-4 ms limits the time available for observation of single molecules.

Second, there is 1D diffusion of the β clamp *on DNA* detected using FRET (Fig. 1C), which we refer to as "β clamp diffusion on DNA." For the β clamp loaded on DNA, we aim to measure how long it takes for the β clamp to diffuse out of the range of FRET (shown in Fig. 1A inset and Fig. 1C). The observed FRET signal is due to complexes of β clamp-DNA that diffuse through a tightly focused laser excitation. Within photon bursts caused by the complexes, motion of the sliding clamp along the DNA would cause fluctuations in the FRET signal.

We analyze diffusion of the β clamp *on DNA* by calculating the autocorrelation of the measured FRET signals (Fig. 1D); the autocorrelation is used to measure how long signals persist before disappearing or returning to equilibrium. At time $\tau=0$, a photon in the FRET channel was detected. The detection of a photon in the FRET channel from a β clamp-DNA complex provides information about that complex. First, the complex must be in the detection volume (Fig. 1A). Second, the β clamp must be near enough to the 5' end of the short section of dsDNA for FRET to occur (Fig. 1A, inset). Subsequent FRET photons will be correlated with the initial photon as indicated by the correlation greater than zero in Fig. 1D. By looking at the decay of the FRET autocorrelation over a large range of time scales, we can determine whether the timescale of β clamp diffusion on DNA out of the range of FRET (~5 nm) is shorter or longer than the plasmid diffusion time (3-4 ms). If the timescale of β clamp diffusion on DNA is longer than the plasmid diffusion time, the persistence of the correlated FRET signal will depend only on how long the plasmid remains in the observation volume; autocorrelations of the FRET signal will reveal only a single decay with the translational diffusion component of the plasmid (black line, Fig. 1C). However, if the timescale of β clamp diffusion on DNA is shorter,

such that the clamp moves in and out of the range of FRET within the plasmid diffusion time, then an additional fluctuation time scale is observed in the FRET autocorrelation (red line, Fig. 1C). The amplitude and timescale of the additional fluctuations depend on the length of dsDNA and on the diffusion constant of the β clamp on DNA.

The timescale of β clamp diffusion on DNA also affects the distributions of E measured over the observation time (Fig. 1E). If the length of dsDNA allows the distance between the D-labeled β clamp and the A-labeled end of the DNA primer to range from below R_0 to above R_0, then a large range of E values will be found as the β clamp diffuses on DNA. If the timescale of β clamp diffusion is longer than the plasmid diffusion time, then E is constant during detected single molecule bursts. The full possible distribution in E values will be observed (black line, Fig. 1E). If the timescale of β clamp diffusion is much shorter than the plasmid diffusion time, then all fluctuations in E are averaged out during the plasmid diffusion time. Rather than a large range in E values, a single averaged E value will be detected (red line, Fig. 1E). If the length of the dsDNA is short, so that E is always near 1, then the observed E distribution (green line, Fig. 1E) will be the same independent of β clamp diffusion. If β clamp is stationary at one position on DNA, then single values of E will be detected. The value of E will depend on the distance between that position and the A-labeled 5' end of DNA.

FRET for labeled *β* clamp and DNA

Details of the labeling positions for the β clamp and for the DNA primers are shown in Fig. 2. In Fig. 2A, molecular models are used to estimate expected distances between Alexa 488 on the sliding clamps and Alexa 647 on the 5' end of the DNA primers. R_0 is 5.1 nm for Alexa488 as D and Alexa 647 as A, based on spectroscopic calculations

(Molecular Probes - Invitrogen, Carlsbad, CA). Considering the fluorophore tethers, we estimated an offset distance of ~2 nm for the D-A at closest approach of the sliding clamp to the 5' end of DNA. In addition to the 2 nm offset at closest approach, the sliding clamp is modeled to have a footprint on the DNA of 4 nm. This leads to the simplified model of the sliding clamp on DNA shown in Fig. 2B.

We fluorescently labeled the β clamp with fluorophore D using a thiol-maleimide reaction (Alexa 488, Materials and Methods). After 2 hours of the labeling reaction, about 20% of the protein was labeled. By trypsin digestion and MS/MS analysis we have established that the labeled residue was Cys180 (out of four possible cysteines). This is in contrast to an earlier report that Cys260 was predominately labeled under similar conditions (Griep and McHenry, 1988). At longer reaction times we found labels at multiple residues—undesirable because it leads to greater uncertainty in FRET expected and more greatly affects the structure of the β clamp.

Four Different lengths of single-stranded DNA oligomer (18, 30, 45, and 90 bases) were labeled at the 5' end with A (Alexa 647). Each oligomer was designed to be complementary to one of two different sites on the single-stranded (ss) M13 plasmid. Eight ssM13 plasmid samples with A-labeled, annealed primers were created in all, each with a short double-stranded (ds) region of DNA. *E. coli* Single stranded binding protein (SSB) or human RP-A was then added which coats the single stranded region and facilitates clamp loading. Purified γ complex, an ATP-driven clamp loader, then loaded the β clamp at the 3' end of the short section of ds DNA. Once loaded, the motion of the β clamp is restricted to be within the length of ds DNA due to the presence of single-stranded binding protein (SSB). We will describe the product of this preparation as a

"loaded clamp" or a "clamp-DNA complex." By comparing the FRET efficiencies, and FRET signal autocorrelations for the primers of different lengths, the diffusion constant of the β clamp on the DNA can be determined. For fast β clamp diffusion a value could be determined; for slow β clamp diffusion, an upper limit could be obtained. For clamps stuck to one end of the DNA oligomers, the relative distance from the 5' end of the various oligomers can be determined using measurement of E.

β Clamp is loaded on DNA

We first tested for loading of the β clamp on DNA, and for the necessity of each reaction component. An initial reaction mixture containing the β clamp, the clamp-loader, and the primed-plasmid coated with SSB but without ATP had no fluorescence bursts with FRET (Fig. S1). The small number of bursts seen had coincident large bursts in the D channel, indicating that those bursts were from aggregates of labeled β clamp. The light detection path was shut off, and 1 mM ATP was added to the reaction mixture. After reopening the light detection path, many bursts with FRET were observed (Fig. S1). The omission of any of the unlabeled components, including the clamp loader, ATP, or SSB, results in a dramatically reduced number of bursts with FRET (data not shown). These data, along with functional assays (Fig. S9, supplementary information), show that clamp is loaded onto the primed DNA region, and can be detected at the single molecule level.

In our experimental conditions, almost all of the fluorescence bursts in our experiments are not from β clamp-DNA complexes. Due to this, we search only for fluorescence bursts that show significant FRET signal. This is an unambiguous signal for a β clamp-DNA complex, but it excludes low E cases as shown in Fig. 3. In order to detect the presence of β clamp-DNA complexes, we use sensitive, reduced background cross-

correlations allowed using ALEX or the equivalent pulsed-interleaved excitation (PIE) (Muller et al., 2005).

Simulations show expected correlations and E histograms

We performed simulations of 1000 s experiments of β clamp proteins sliding on short DNA regions which are themselves diffusing into and out of a confocal detection volume (Figure 3). The diffusion time of the primed plasmids or "observation time" was 3 ms. There were 5 sets of simulations performed with different β clamp diffusion constants from $D = 10^{-11}$ cm^2/s to $D = 10^{-15}$ cm^2/s. At each value of D, a simulation was performed for each primer length: 18, 30, 45, and 90 bases. FRET autocorrelation functions for different diffusion constants were extracted using purified fluorescence correlation spectroscopy (PFCS; Fig. 3), with similar parameters as used for the experiments. For $D > 10^{-15}$ cm^2/s, there is a clear difference in all cases between the curves for the 18mer (black), 30mer (red), 45mer (green), and 90mer (blue). These correlation amplitudes are large because E oscillates randomly between the extreme values of 0 and 1. For $D \geq 10^{-13}$ m^2/s, two time scales for the fluctuations are clearly visible, most dramatically seen in the case of the 90mer. For $D = 10^{-15}$ cm^2/s, the FRET fluctuations cause by β clamp diffusion occur on time scales longer than the plasmid diffusion time. Since the observation time for each molecule is limited by the plasmid diffusion time, only the plasmid diffusion is visible for $D \leq 10^{-15}$ m^2/s. $D = 10^{-14}$ m^2/s is a marginal case, where two time scales are not readily apparent in a single curve, but the effective time scale of the fluctuations decreases with increasing primer length.

These fluctuations in FRET also affect the expected histograms in energy transfer

efficiency E (Figure 3). For slow β clamp diffusion ($D = 10^{-15}$ cm^2/s, Figure F3B), E

will remain constant during the observation time. The histograms expected are similar

for the 18mer, 30mer, 45mer, and 90mer DNA oligomers, each showing a significant

peak at high E. An additional peak is expected at low E for all of the oligomers except

for the 18mer. This peak is excluded by searching only for bursts that show significant

FRET signal. For faster diffusion of β clamp on DNA, fluctuations in E are averaged

during the observation time. In our experimental conditions, this leads to lower observed

average E and narrower E distributions for longer DNA primers. The decrease in

observed average E becomes more dramatic as the β clamp diffusion is increased from D

= 10^{-14} m^2/s to D = 10^{-12} m^2/s. The decrease occurs concurrently with a narrowing of the

E histogram.

β Clamp stays at 3' end in presence of SSB

E. coli single-stranded binding protein (SSB) coats the single-stranded region of the

plasmid, and enhances loading of β clamp (Fradkin and Kornberg, 1992). In the presence

of SSB, we found values for E significantly lower than expected for the 30mer (Figures

4A and 4B, and supplementary figures S2-S4). Rather than the small change in E shown

in Figure 3, a comparatively large shift was seen. For the 45mer and 90mer, very few

bursts were observed. For the observed bursts, there was a wide range in E observed. In

the experiments for Figures 4, S2-S4, there is three times more DNA than β clamp.

Based on cross-correlation analysis discussed below, the largest fraction of DNA loaded

under any of the conditions used is 1%, usually much less. There is negligible loading of

multiple β clamps in these conditions.

There are three possible explanations for our experimental observations of E to be different from our estimates of expected E in Figure 3. First, as in many other single molecule FRET measurements (Ha et al., 2002; Kapanidis et al., 2005), our experimental E measurements are not calibrated. Currently, these values can be used to compare relative distances, but not absolute distances. Since there are far fewer bursts for the 45mer and 90mer than for the 30mer, this would suggest that fluctuations in distance within the observation time are leading to averaging of E, as in Figures 3D, F, and H. However, no corresponding FRET fluctuations were evident in the FRET autocorrelations (see below). Due to signal-to-noise in our measurements, we cannot exclude the case in Figure 3D, with $D = 10^{-14}$ m^2/s.

A second possibility also supposes poor calibration of E, but also invokes varying β clamp loading rates for different DNA oligomers. The 45mer and 90mer could have much lower loading efficiency due to sequence. This is unlikely since we performed these experiments on two sets of oligomers with difference sequences and saw similar results for each. Additionally, using cross-correlations as discussed below, we measure significant loading of the β clamp on the 45mer and 90mer.

A third explanation is that the β clamp remains stationary at the 3' end of the DNA. The lower E observed for the 30mer corresponds to the larger distance between the A-labeled 5' end of DNA and the D-labeled β clamp than for the 18mer. For the even longer distances encountered with the 45mer and 90mer, there is no FRET and therefore no detected bursts. The few bursts observed are due a small number of β clamps that occasionally become free from the 3' end.

In order to clearly differentiate between these possibilities, we replaced SSB with human version of SSB (RP-A) to coat the single stranded region of the DNA as done in (Kelman et al., 1998). Since the only other proteins present in solution are SSB and the γ complex clamp loader, it is likely that SSB was involved in the 3' interaction. By replacing SSB with Human RP-A, we could possibly prohibit or greatly reduce any interaction with SSB. Our results demonstrate that this indeed disrupts the interaction. Significant changes in the number of bursts with FRET and in the distribution of E are observed for the 30mer and 45mer (Figures 4C-D). The E distribution measured for the 30mer nearly matches the E distribution measured for the 18mer. A much larger number of events were detected for the 45mer than in the presence of SSB, and the distribution in E is broader than those found in the 18mer and 30mer. More bursts with FRET are detected in the case of the 90mer with RP-A, but the change is not as dramatic. The simultaneous increases in the number of bursts showing FRET and in the measured E indicate that using RP-A frees the β clamp from the 3' end.

Comparing the E histograms using RP-A with the simulation results, there must be some diffusion of the β clamp on DNA within the observation time. The distribution for the 45mer has a peak at lower E than for the 30mer. For slow β clamp diffusion, with $D \leq 10^{-15}$ cm^2/s, there should be a distribution peak at high E (near 1) for all of the oligomers. We do not observe that for the 45mer or the 90mer. This implies a diffusion constant of D > 10^{-15} m^2/s.

Lowering NaCl concentration and use of human RP-A slows removal of clamps from DNA

Kinetic information on the reaction is extracted by counting the number of complexes (bursts with FRET) observed as a function of time. For each of the experiments, the ATP is added to the reaction mixture on ice. The reaction mixture is transferred to a heated chamber (held 35±2ºC), and recording of the experiment starts. Figure 5 shows the number of fluorescence bursts with FRET detected as a function of time for the same experiments shown in Figures 4 and S2. With SSB, the change in temperature causes a new equilibrium to be reached, with a much lower fraction of clamps loaded. This new equilibrium is nearly reached in 15 minutes with 50 mM added NaCl, whereas the new equilibrium is reached much more slowly in low NaCl conditions. The decrease in the number of bursts with FRET observed is not likely due to consumption of ATP since the concentration of β clamp and γ complex are low (<1 nM). Also, in other experiments where concentration of β clamp in 25 times higher, and the DNA is 3 times lower, the kinetics of this decrease in the number of bursts is the same, within error (Figure S5).

When using RPA, the number of events observed increases dramatically over time with longer primers. Freeing the β clamp from the 3' end appears to have an important effect on the efficiency of the clamp unloading pathway of the clamp loader complex. If the β clamp is free to move around the dsDNA region, it is not available for unloading. β clamps then accumulate on the DNA, allowing for many more β clamp-DNA complexes to be observed.

Autocorrelation analysis indicates slow β clamp diffusion on DNA

Fluctuations in distance between the D-labeled β clamp and A-labeled 5' end of the DNA

primer causes strong fluctuations in the FRET efficiency E, ranging from 0 to 1. We

extracted autocorrelations of the FRET signal using purified fluorescence correlation

spectroscopy (PFCS) (Laurence et al., 2007). We studied the effects of varying the DNA

oligomer lengths on the autocorrelation of the FRET signal, and compared them to

expected autocorrelations from simulations. We determine that the time scale of β clamp

diffusion on DNA is similar to or slower than the observation time of 3-4 ms, leading to a

limit on the clamp diffusion constant of $D \leq 10^{-14}$ cm^2/s.

The measured FRET autocorrelation curves are shown in Fig. 6. There is no

significant difference found between the correlation curves for different primer lengths,

matching the simulation results for $D = 10^{-15}$ cm^2/s and $D = 10^{-14}$ cm^2/s. The

variability of the data due to noise and photobleaching (see cross-correlations below)

prevent distinguishing these two cases. An FCS model with a single diffusing component

fits well to all experiments. To exclude the possibility that the fluctuations are simply on

time scales shorter than the 25 μs minimum resolution shown in Fig. 6, we also

calculated FRET autocorrelations that corrected for the laser switching on the 25 μs time

scale used for ALEX (not shown). In this case, there is no evidence of primer-dependent

fluctuations down to 10^{-7} s. We also found no evidence of fluctuations using Donor-

FRET cross-correlations (not shown). Hence, we conclude that the fluctuations are

occurring on time scales longer than our observation time, and $D \leq 10^{-14}$ cm^2/s. Our

ability to distinguish between the cases with $D = 10^{-15}$ cm^2/s and $D = 10^{-14}$ cm^2/s is

hampered by observed photobleaching of the donor and acceptor fluorophores (see below).

Loading multiple clamps indicates weak clamp-SSB interaction

We also attempted to observe fluctuations of the FRET signal related to distance fluctuations using conditions where multiple β clamps are loaded (Figure S6). As discussed in the Methods, we used 10 nM labeled β clamp in the presence of 1 nM plasmid. This creates a situation where the 18mer was saturated with one clamp per DNA, but longer oligomers such as the 90mer were not. Two or more clamps were present on these primers, freeing at least one of the clamps from the 3' end. This would allow distance fluctuations to be observed if they were on time scales faster than the plasmid diffusion time. Again, no evidence was seen for FRET fluctuations.

The results of these experiments are consistent with our finding that, in the presence of SSB, the β clamp remains at the 3' end of DNA. While loading multiple β clamps, we would expect to see many more bursts with FRET in the case of 90mer. Increasing the loading to saturation, we would expect to see a similar number of bursts with FRET in 18mer and 90mer. This was observed (Fig. S6B).

Cross-correlation analysis reveals binding when there is no FRET

FRET reveals loading of the β clamp to DNA for the short DNA oligomers (18mer, 30mer, and 45mer under certain conditions). However, for longer oligomers such as the 90mer, there are very few bursts showing significant FRET under any of the experimental conditions. We use cross-correlation analysis to reveal the presence of β clamp-DNA complexes (Figure 7, Table 1). We use a cross-correlation between the Donor channel

and the Acceptor channel excited by the excitation laser. We exclude Acceptor signal excited by the Donor excitation laser, greatly reducing contaminating leakage of signals (Muller et al., 2005). Such cross-correlations are sensitive under conditions where FRET efficiency E is low, and are complementary to our analysis above. As seen in Figure 7, significant cross-correlation signals are able to be extracted, and indicate binding even when no FRET occurs. In Table 1, the extracted molecular occupancies for the complex are shown for our experiments. Since FRET reduces or eliminates the signals of the complex in the Donor channel, these occupancies are reduced for the short primers (18mer and 30mer). However, for the 45mer and 90mer, the full concentrations of complexes are detected. Note that, for the longer primers, there is more efficient loading of β clamp in the case of RP-A than for SSB, the opposite of what is seen for the 18mer. Using analysis of bursts with FRET, Figure 5 shows this to be true for the 30mer as well.

Additional evidence for binding in cases without FRET is provided by single molecule FCS analysis of the donor fluorescence (Laurence et al., 2007). Due to the much greater size of the DNA plasmid than the β clamp dimer, the diffusion time of the β clamp on DNA is expected to be significantly longer than the β clamp alone. The histograms of fitted diffusion times for single molecule fluorescence bursts in the donor channel indicate formation of β clamp-DNA complexes, with similar trends as seen in the cross-correlation analysis (Figure S7).

Cross-correlation analysis reveals fluorophore photobleaching

Evidence of fluorophore photobleaching is provided using cross-correlations. Mathematically, a cross-correlation compares signals in one channel with a time-shifted version of the signals in a second channel. By comparing cross-correlations with varying

time shifts or lags, one measures how long a signal persists in the second channel after a signal is detected in the first channel (Schwille et al., 1997). For a random process, a correlation time may be defined roughly as the time it takes for the cross-correlation value to decrease by a factor of 2. Unlike with an autocorrelation, it is possible that the cross-correlation of the signal to be different for positive or negative values of time lag. Such a difference in positive or negative time lags can only occur when there is a time asymmetry in the dynamical process observed. For the near equilibrium conditions we are studying, fluorophore photobleaching is almost certainly the cause. If the acceptor were to photobleach before the donor, the "acceptor preceding donor" cross-correlation would persist longer than the "donor preceding acceptor" cross-correlation. If Figure S8, it can be seen that, when there is no FRET (for example with the 90mer), the "donor preceding acceptor" correlations have longer correlation times, indicating that the donor photobleaches before the acceptor. In high FRET cases, for example with the 18mer, the "acceptor preceding donor" correlations have longer correlation times, indicating that the acceptor photobleaches before the acceptor. The photobleaching occurs on times scales such that they do not interfere with any of our results, except that they prevent us from distinguishing between $D = 10^{-15}$ cm$^2/$s and $D = 10^{-14}$ cm$^2/$s. Further experiments on immobilized complexes will be required to directly observe the movement of the β clamp on DNA.

Discussion

The question that we have endeavored to answer is to what extent the DNA sliding clamps freely slides along DNA? The answer is that it moves quite slowly, but not slowly enough to produce a significant drag on the DNA polymerase.

The solution based measurements have allowed us to set an upper limit for the diffusion constant of the β clamp on DNA several orders of magnitude below free diffusion. If surface-immobilized or gel-immobilized single-molecule measurements were performed first, the immobilization strategy would lead to doubts about such a dramatically lower diffusion constant. With these results, measurements on immobilized molecules will be more believable.

Our measurements suggest that the actual diffusion constant is between 10^{-14} m^2/s and 10^{-15} m^2/s, that is, only a little faster than the very slowest limit. In a computational study, involving molecular dynamics simulations, we have examined the hypothesis that many residues form salt bridges with the DNA and found this to be likely: during several nanoseconds of simulation there were always at least three (up to eight) salt bridges between arginine residues and the DNA phosphate groups, suggesting a mechanism for intermolecular stickiness or friction (manuscript in preparation).

This discovery of slow diffusion highly significant, for it may change the understood role of the clamp; rather than acting as a tether, the clamp may also act as a placeholder. Intermolecular stickiness or friction may limit the distance that the clamp can move between bases or after being loaded. This may help in switching between polymerases and other accessory proteins necessary for DNA replication and repair.

Even with this relatively slow diffusion constant, diffusion of the clamp may be problematic for several processes in DNA replication and repair. Other strategies appear to be employed for keeping the clamp in place. A separate study suggests that the clamp interacts directly with 3' end of DNA (Roxana et al., submitted). We have detected that the β clamp remain at the 3' end after loading, when in the presence of SSB. Although

this interaction is reasonable mechanistically, allowing the β clamp to remain in place, we have not determined the precise nature of this interaction. The interaction is not strong, since it must allow for loading of additional β clamps, unloading, and attachment of DNA polymerases.

We propose three possible explanations for this interaction. First, there could be direct binding of the β clamp to SSB. Second, there could be a β clamp-DNA interaction that holds the β clamp in place in the presence of SSB (Roxana et al., submitted), but the interaction is disrupted by RP-A, which may interact more directly with dsDNA-ssDNA junctions, and prevent this association. An intriguing observation is that adding RP-A causing some quenching of the fluorescence from the acceptor label at the 5' end of DNA. Third, the interaction between the β clamp and SSB at the 3' end could be mediated by the γ clamp loader complex. The γ complex interacts with β clamp and SSB (Kelman et al., 1998), and could mediate an interaction. However, upon ATP hydrolysis, the γ complex is thought to be ejected from the dsDNA-ssDNA junction (Turner et al., 1999). It is possible that ATP hydrolysis doesn't fully eject the clamp, but only greatly weakens the interaction between clamp and clamp loader. The interaction with the partially ejected γ complex would have to be weak enough gone after gel filtration. Regardless of the precise mechanism to be determined, the β clamp now appears to remain at the 3' end until a DNA polymerase attaches.

Experimental Procedures

Preparation of DNA substrates, cloning of β clamp, and fluorescent labeling of β clamp are as described in (Laurence et al., 2007).

Replication Activity Assays

Activity of the labeled β clamp was assayed by the stimulation of nucleotide incorporation by the core polymerase (αεθ subunits). The reaction mixture contained core polymerase (5 nM), γ complex (1.6 nM), SSB (420 nM tetramer), primed M13mp18 ssDNA (1.1 nM), 60 μM each of dATP, dCTP, and dGTP, 20 μM α-^{32}P TTP, 1 mM ATP, and 10 mM $MgCl_2$ in 25 μL Reaction Buffer (final volume). The Reaction Buffer is 20 mM Tris-HCl (pH 7.5), 0.1 mM EDTA, 5 mM DTT, 4% glycerol (v/v), and 40 μg/ml BSA. Replication was initiated upon addition of β clamp (0-32 nM titration) and incubated at 37°C for 5 min. Reactions were quenched upon addition of 25 μL 1 % SDS, 40 mM EDTA. Quenched reactions were spotted onto DE81 (Whatman) filters, then washed and quantitated by liquid scintillation as described (Studwell and O'Donnell, 1990). Products were separated on a 0.8% agarose gel and visualized by PhorphorImager (GE Healthcare).

Trypsin digestion and MS analysis

Tris buffer (50 μl, 1 M, pH 8) was added to the solution of fluorescently labeled β-clamp (5 μM, 450 μl) to adjust pH 8. Sequencing grade modified trypsin (Promega) was added to the protein solution to make final trypsin/protein ratios of 1:20. The mixture was heated to 37°C and the digestion reaction was monitored by removing 10 μl of reaction mixture and analyzing the peptide profile by reverse-phase HPLC at 220 and 490 nm. Upon the completion of digestion reaction, the 490 nm absorbing peptides were purified using reverse-phase HPLC and the purified peptides were analyzed using ES-MS.

   MS analysis was performed at the Vincent Coates Foundation Mass Spectrometry Laboratory, Stanford University Mass Spectrometry (http://mass-spec.stanford.edu).

Peptide fractions collected from HPLC were diluted with an equal volume of 0.2% formic acid in methanol. Aliquots (5 uL) were analyzed by static nanospray infusion using an Advion NanoMate (Advion Biosciences, Ithaca, NY); 0.3 psi, 1.45 kV. MS and MS/MS data were collected on a Q-Tof API US hybrid quadrupole-time of flight mass spectrometer (Micromass-Waters Corp., Milford, MA). Peptide sequence and modifications were confirmed by comparing the observed and theoretical peptide fragment ions. In particular, the mass and position of the attached dye was confirmed to the specific amino acid by ions from both the b- and y-ion series.

Loading of β clamp on DNA

Loading of the β clamp is performed as in (Laurence et al., 2007). For the multiple β clamp loading experiments, a 100 μl reaction mixture was formed in a 20 mM 7.5 pH Tris buffer with 0.1 mM EDTA, 4% glycerol, 40 μg/ml BSA, 8 mM $MgCl_2$, and 50 mM NaCl. 40 fmol of M13 plasmid with annealed DNA oligomer is added with 220 pmol of single-stranded binding protein (SSB). 0.4 pmol of γ clamp loading complex and 1 pmol of β-clamp (labeled monomer) are then added. Finally ATP is added to a final concentration of 1 mM. 50 μl of this reaction mixture is placed in well formed in a cell incubation chamber (WillCo-dish GWSt-3522, WillCo Wells BV, Amsterdam, The Netherlands) with silicone gasket (Grace biolabs). The solution is covered with a coverslip and is heated from room temperature to 35 ± 2 ºC over a period of 2 minutes using a microscope-based heater (Warner Instruments, Hamden, Connecticut). ALEX-based single-molecule spectroscopy is then performed for the specified times (20 minutes) at 35 ± 2 ºC.

For the experiments with lower β clamp concentration, a 50 μl reaction mixture was formed in a 20 mM 7.5 pH Tris buffer with 0.1 mM EDTA, 4% glycerol, 40 μg/ml BSA, 8 mM $MgCl_2$. NaCl is added to a concentration of 50 mM or 0 mM depending on the experiment. 60 fmol of M13 plasmid with annealed DNA oligomer is added with 330 pmol of SSB (or human RP-A). 100 fmol of γ clamp loading complex and 40 fmol of β-clamp (labeled monomer) are then added. Finally ATP is added and observation continues as described above. ALEX-based single-molecule spectroscopy is then performed for the specified times (75-180 minutes) at 35 ± 2 ºC.

Single-molecule fluorescence spectroscopy of diffusing species

These are performed as described in (Laurence et al., 2007), except that the OD 1.2 neutral density filter is removed from the Donor channel for all measurements except for the multiple β clamp loading experiments.

Purified Fluorescence Correlation Spectroscopy (FCS)

Extracting the FRET autocorrelations from our measurements is complicated by leakage of D signal into the A channel and direct excitation of A fluorophores by the D excitation laser. Most of the signal in the FRET channel does not come from β clamp-DNA complexes. FRET bursts from β clamp loaded onto primed DNA plasmids are infrequent, especially in experiments with longer primers. Although the FRET bursts are much brighter than the other signals (except for the bursts from aggregates), it is not clear *a priori* how much of a FRET autocorrelation signal would come from β clamp-primed plasmid complexes and how much would come from other sources.

We use purified fluorescence correlation spectroscopy (PFCS) to obtain FRET autocorrelation signals only from bursts from β clamp-DNA complexes (Laurence et al.,

2007). Bursts in the FRET channel are sorted into bursts that have a coincident burst in the D channel (indicating a β clamp aggregate) and those that do not (indicating a β clamp-primed plasmid complex). For each burst, a region of interest for calculating correlations is chosen 100 ms before the burst and 100 ms after the burst. As long as there is no β clamp aggregate burst within this expanded region of interest, the FRET autocorrelation for this region is added to the final FRET autocorrelation for all bursts. The burst selection allows only the relevant signals to contribute, and the 100 ms expansion of the correlation region allows standard FCS models to be applied to the result.

We perform FCS analysis of the data collected using ALEX data with a minimum time lag of 25 microseconds (to match the alternation period) and maximum time lag of 10 s. The data are fit using the model, $C_{\text{diff}}(\tau) = 1/N(1 + \tau/\tau_D)$ for diffusion.

For the autocorrelation of the FRET signal, the total observed correlations are calculated by multiplying the diffusion autocorrelation with the simulated FRET correlations due to the movement of the sliding clamp on the DNA (next section),

$$G_{\text{total}}(\tau) = 1 + C_{\text{diffusion}}(\tau) C_{\text{FRET}}(\tau).$$

1D diffusion simulations

Simulation of translational diffusion in a confocal detection volume was performed as described in (Laurence et al., 2004), with diffusion time of entire complex set to 3 ms. Simulations of the expected FRET intensity fluctuations were added by simulating diffusion of a particle in a 1D potential well. The size of the potential well was chosen to correspond to dsDNA regions of various lengths (18, 30, 45, and 90 base pairs),

subtracting out the β clamp footprint of approximately 12 base pairs. The sliding clamp

is assumed to undergo free 1D diffusion without sticking at either end. The movement of

the β clamp-DNA complex via 3D diffusion is simulated in time steps of $\Delta t_{complex} = 1$ μs.

During this interval, photon excitation events are generated via a simulated Poisson

process where the rate is determined by the 3D position of the complex in the confocal

detection volume. Between each photon excitation event, there is a time between

excitation of $\Delta t_{\beta\text{-DNA}}$. The distance that the β clamp diffuses on DNA during this interval

is determined by a simulated Gaussian random variable x which satisfies

$\langle x^2 \rangle = 2D\Delta t_{\beta-\text{DNA}}$. Reflecting boundary conditions are imposed to keep the β clamp on

the short DNA track. D is the diffusion constant as described earlier, and the values were

chosen from $D=10^{-11}$ m^2/s to $D=5\times10^{-15}$ m^2/s.

Acknowledgments

Figures

Figure 1: (a) Single-molecule measurements of fluorescence resonance energy transfer

(FRET) on freely diffusing molecules are used to extract information about the

movement and interactions of the β sliding clamp of *E. coli* (β clamp) on DNA. A β

clamp labeled with a donor fluorophore (D) is loaded onto a short section of double-

stranded DNA. The short section of DNA is formed by annealing a short DNA primer labeled with an acceptor fluorophore (A) at the 5' end to a single-stranded plasmid, which is then coated with single-stranded binding protein (SSB, small circles). Two types of diffusion are present in these experiments: the diffusion of the entire protein-DNA complex through optical detection volume ("plasmid diffusion") (b) and the diffusion of the β clamp on the double-stranded DNA ("β clamp diffusion on DNA") (c). (d) Fluorescence correlation spectroscopy (FCS) of the FRET signal may be used to determine the time scale of β clamp diffusion. If the β clamp diffusion is faster than the plasmid diffusion, then two times scales are observed in the FRET autocorrelation function (red curve), and both time scales may be extracted. However, if β clamp diffusion is slower, only the plasmid diffusion is seen (black curve). In this case, only a lower limit on the β clamp diffusion time is obtained. (e) These two cases (fast and slow β clamp diffusion time) are revealed in the distribution of measured values of FRET efficiency E for the transits of single β clamp-DNA complexes. If the β clamp diffusion time is faster, then a single E value is measured (red curve). However, if the β clamp diffusion time is slower, then a wide distribution of E values from $E=0$ to 1 are measured (black curve). For a short primer that restricts the β clamp to regions within FRET range, both cases result in only high E values (green curve).

Figure 2: FRET efficiency values expected in our experiments. (a) The β clamp is labeled with Alexa 488 acting as donor at available cysteines. The smaller fluorophore was chosen to label the β clamp in order to minimize potential effects. Analysis of trypsin digestions indicate that the C180 is preferentially labeled (see supplemental information). (b) We model the β clamp as a ring with a 4 nm width (along the DNA)

labeled with D 2 nm from the center of the ring. (c) Four different lengths of DNA primers are used in our experiments (18, 30, 45, and 90 bases), each with a different range of possible E values. The 4 nm width of the β clamp translates into a "footprint" of 12 base pairs on the double-stranded DNA. E as a function of D-A separation is shown. The limits for individual primers are shown in red.

Figure 3: Expected FCS curves and histograms of energy transfer efficiency E for different values of the diffusion constant D of the β clamp on DNA. These results are from simulations considering both diffusion of the β clamp on DNA as well as diffusion of the entire plasmid through the optical detection volume. 1000 s photon streams are generated, and undergo the same data analysis procedures as the experimental data. In each case, the black line is for the 18mer, red line for the 30mer, green line for the 45mer, and blue line for the 90mer. **A**. Correlations expected for $D = 10^{-15}$ m^2/s. **B**. E histogram for $D =10^{-15}$ m^2/s. **C** and **D**. Same as A and B, but for $D =10^{-14}$ m^2/s. **E** and **F**. $D =10^{-13}$ m^2/s. **G** and **H**. $D =10^{-12}$ m^2/s.

Figure 4: Histograms showing number of observed complexes with FRET efficiency E as a function of DNA oligomer length (annealed to site 1 of the DNA plasmid). Higher E indicates shorter distances. These E Histograms obtained from experiments on β-clamp DNA complexes under varying conditions. Black: 18mer; red: 30mer; green: 45mer. Histograms are normalized by area. Only histograms with a significant number of events and well defined peaks are shown. Additional histograms for the 90mer and 45mer (with SSB) are shown in the supplemental information; these histograms have fewer events, but show broad distributions in E. Conditions. A. *E. coli* single-stranded binding protein (SSB) with 50 mM added NaCl (top) and 0 mM added NaCl (bottom). These histograms

provide evidence for the β clamp sticking to the 3' end of DNA (illustration). B. Human

RP-A and 50 mM added NaCl (top) and 0 mM added NaCl (bottom). Use of Human RP-

A releases the β clamp from the 3' end (illustration).

Figure 5: Kinetic data of loading/unloading monitored by counting single molecule

bursts with significant FRET counts upon addition of ATP at 0 minutes; the temperature

is increased from being on ice to an incubation chamber held 35±2ºC. The number of

single molecule bursts showing FRET is shown in 15 minute increments. Time periods

with large aggregates crossing the detection volume are excluded. For site 1 on the DNA

plasmid, the 18mer is shown in black, the 30mer in red, and 45mer in cyan. Experiments

were 180 minutes. For site 2, the 18mer is shown in green, the 30mer in blue, and the

45mer in magenta. Experiments were 90 minutes. Conditions. A. SSB, 50 mM added

NaCl. B. SSB, 0 mM added NaCl. C. Human RP-A, 50 mM added NaCl. D. Human

RP-A, 0 mM added NaCl.

Figure 6: No significant difference is found between the correlation functions obtained

in experiments with different primer lengths and different conditions.   Black: 18mer; red:

30mer; green: 45mer; blue: 90mer. Conditions. A. *E. coli* single-stranded binding protein

(SSB) and 50 mM added NaCl. B. SSB and 0 mM added NaCl. C. Y-RPA and 50 mM

added NaCl. D. RPA, the human homolog to SSB (RPA), and 0 mM added NaCl. In the

supplemental information, correlation analysis that corrects for ALEX-induced

fluctuations indicates that there are no primer-dependent fluctuations down to 10^{-7} s.

Figure 7: Cross-correlation between Donor channel and Acceptor channel (excited by

acceptor excitation laser) reveals β clamp-DNA complexes when FRET does not occur.

A global fit of the cross-correlations and autocorrelations was used to extract diffusion

time scales and molecular occupancies of free and bound species. A. Red and black lines: cross-correlations for experiment with 90 base DNA primer and using SSB to coat the single-stranded DNA. Green line: fit. Blue and Cyan lines: cross-correlations for experiment with 90 base DNA primer at site 1 without adding ATP. B. Black: autocorrelation of Donor channel. Green: fit. Red: autocorrelation of Acceptor channel. Blue: fit. C. Molecular occupancy of β clamp-DNA complex for each primer and various experimental conditions. The x-axis is the length of the DNA primer. Black: *E. coli* single-stranded binding protein (SSB) and 50 mM added NaCl. Red: SSB and 0 mM added NaCl. Green:RPA and 50 mM added NaCl. Blue: RPA and 0 mM added NaCl.

References

Fay, P.J., Johanson, K.O., McHenry, C.S., and Bambara, R.A. (1981). Size classes of products synthesized processively by DNA polymerase III and DNA polymerase III holoenzyme of Escherichia coli. J Biol Chem *256*, 976-983.

Fradkin, L.G., and Kornberg, A. (1992). Prereplicative complexes of components of DNA polymerase III holoenzyme of Escherichia coli. J Biol Chem *267*, 10318-10322.

Griep, M.A., and McHenry, C.S. (1988). The dimer of the beta subunit of Escherichia coli DNA polymerase III holoenzyme is dissociated into monomers upon binding magnesium(II). Biochemistry *27*, 5210-5215.

Gulbis, J.M., Kelman, Z., Hurwitz, J., O'Donnell, M., and Kuriyan, J. (1996). Structure of the C-terminal region of p21(WAF1/CIP1) complexed with human PCNA. Cell *87*, 297-306.

Ha, T., Rasnik, I., Cheng, W., Babcock, H.P., Gauss, G.H., Lohman, T.M., and Chu, S. (2002). Initiation and re-initiation of DNA unwinding by the Escherichia coli Rep helicase. Nature *419*, 638-641.

Indiani, C., McInerney, P., Georgescu, R., Goodman, M.F., and O'Donnell, M. (2005). A sliding-clamp toolbelt binds high- and low-fidelity DNA polymerases simultaneously. Mol Cell *19*, 805-815.

Johnson, A., and O'Donnell, M. (2005). Cellular DNA replicases: components and dynamics at the replication fork. Annu Rev Biochem *74*, 283-315.

Kapanidis, A.N., Lee, N.K., Laurence, T.A., Doose, S., Margeat, E., and Weiss, S. (2004). Fluorescence-aided molecule sorting: analysis of structure and interactions by alternating-laser excitation of single molecules. Proc Natl Acad Sci U S A *101*, 8936-8941.

Kapanidis, A.N., Margeat, E., Ho, S.O., Kortkhonjia, E., Weiss, S., and Ebright, R.H. (2006). Initial transcription by RNA polymerase proceeds through a DNA-scrunching mechanism. Science *314*, 1144-1147.

Kapanidis, A.N., Margeat, E., Laurence, T.A., Doose, S., Ho, S.O., Mukhopadhyay, J., Kortkhonjia, E., Mekler, V., Ebright, R.H., and Weiss, S. (2005). Retention of transcription initiation factor sigma70 in transcription elongation: single-molecule analysis. Mol Cell *20*, 347-356.

Kelman, Z., Yuzhakov, A., Andjelkovic, J., and O'Donnell, M. (1998). Devoted to the lagging strand-the subunit of DNA polymerase III holoenzyme contacts SSB to promote processive elongation and sliding clamp assembly. Embo J *17*, 2436-2449.

Kong, X.P., Onrust, R., O'Donnell, M., and Kuriyan, J. (1992). Three-dimensional structure of the beta subunit of E. coli DNA polymerase III holoenzyme: a sliding DNA clamp. Cell *69*, 425-437.

Laurence, T.A., Kapanidis, A.N., Kong, X.X., Chemla, D.S., and Weiss, S. (2004). Photon arrival-time interval distribution (PAID): A novel tool for analyzing molecular interactions. J Phys Chem B *108*, 3051-3067.

Laurence, T.A., Kwon, Y., Yin, E., Hollars, C.W., Camarero, J.A., and Barsky, D. (2007). Correlation Spectroscopy of Minor Fluorescent Species: Signal Purification and Distribution Analysis. Biophys. J. *92*, 2184-2198.

Lopez de Saro, F.J., and O'Donnell, M. (2001). Interaction of the beta sliding clamp with MutS, ligase, and DNA polymerase I. Proc Natl Acad Sci U S A *98*, 8376-8380.

Maga, G., and Hubscher, U. (2003). Proliferating cell nuclear antigen (PCNA): a dancer with many partners. J Cell Sci *116*, 3051-3060.

Majka, J., and Burgers, P.M. (2004). The PCNA-RFC families of DNA clamps and clamp loaders. Prog Nucleic Acid Res Mol Biol *78*, 227-260.

Muller, B.K., Zaychikov, E., Brauchle, C., and Lamb, D.C. (2005). Pulsed interleaved excitation. Biophysical Journal *89*, 3508-3522.

O'Donnell, M.E., and Kornberg, A. (1985). Complete replication of templates by Escherichia coli DNA polymerase III holoenzyme. J Biol Chem *260*, 12884-12889.

Schwille, P., Meyer-Almes, F.J., and Rigler, R. (1997). Dual-color fluorescence cross-correlation spectroscopy for multicomponent diffusional analysis in solution [see comments]. Biophysical Journal *72*, 1878-1886.

Smiley, R.D., Zhuang, Z., Benkovic, S.J., and Hammes, G.G. (2006). Single-molecule investigation of the T4 bacteriophage DNA polymerase holoenzyme: multiple pathways of holoenzyme formation. Biochemistry *45*, 7990-7997.

Stryer, L. (1995). Biochemistry, 4th edition (New York: W.H. Freeman and Company).

Studwell, P.S., and O'Donnell, M. (1990). Processive replication is contingent on the exonuclease subunit of DNA polymerase III holoenzyme. J Biol Chem *265*, 1171-1178.

Turner, J., Hingorani, M.M., Kelman, Z., and O'Donnell, M. (1999). The internal workings of a DNA polymerase clamp-loading machine. Embo Journal *18*, 771-783.

Vivona, J.B., and Kelman, Z. (2003). The diverse spectrum of sliding clamp interacting proteins. FEBS Lett *546*, 167-172.

Yao, N., Hurwitz, J., and O'Donnell, M. (2000). Dynamics of beta and proliferating cell nuclear antigen sliding clamps in traversing DNA secondary structure. J Biol Chem *275*, 1421-1432.

Yao, N., Turner, J., Kelman, Z., Stukenberg, P.T., Dean, F., Shechter, D., Pan, Z.Q., Hurwitz, J., and O'Donnell, M. (1996). Clamp loading, unloading and intrinsic stability of the PCNA, beta and gp45 sliding clamps of human, E. coli and T4 replicases. Genes Cells *1*, 101-113.

Figure 1
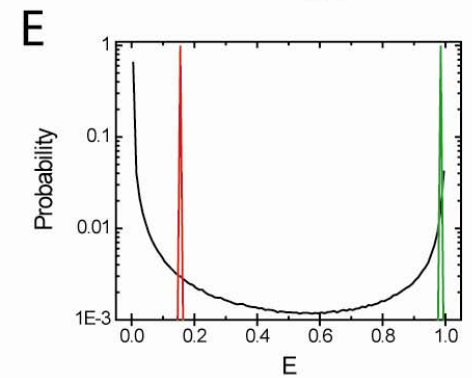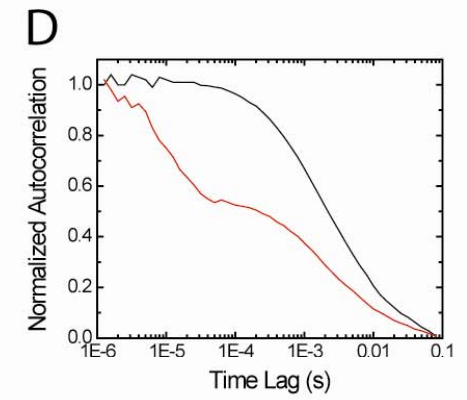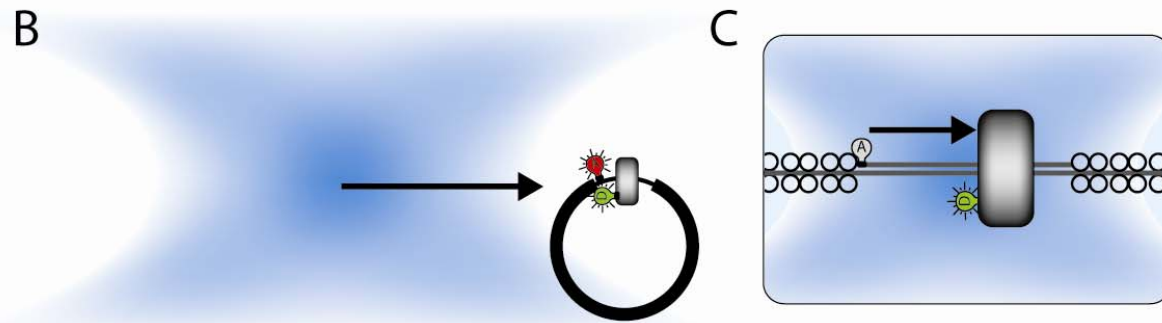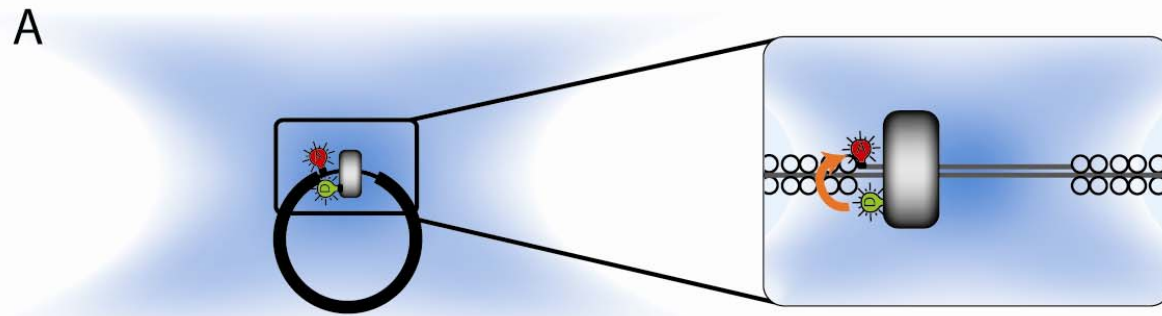
Figure 2
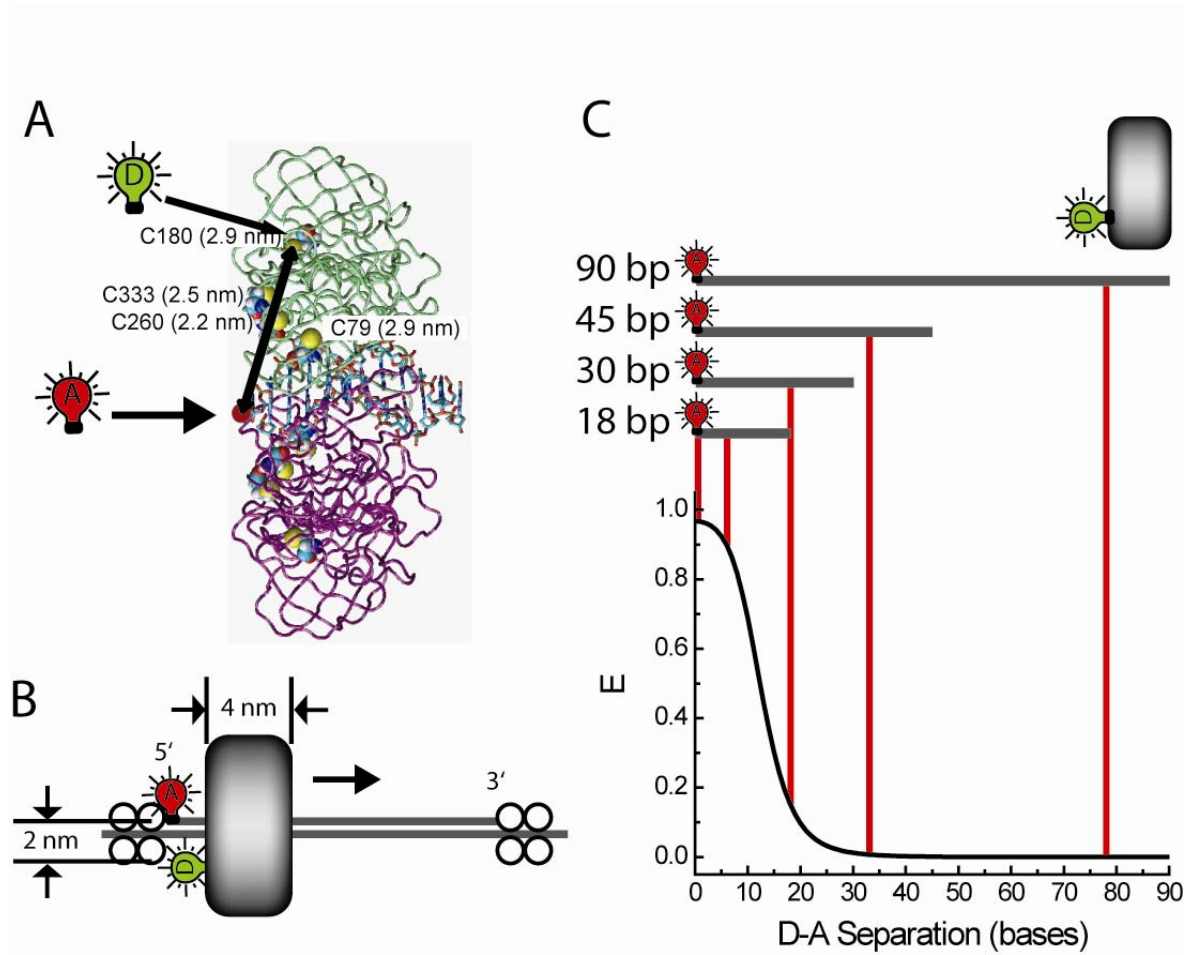
Figure 3
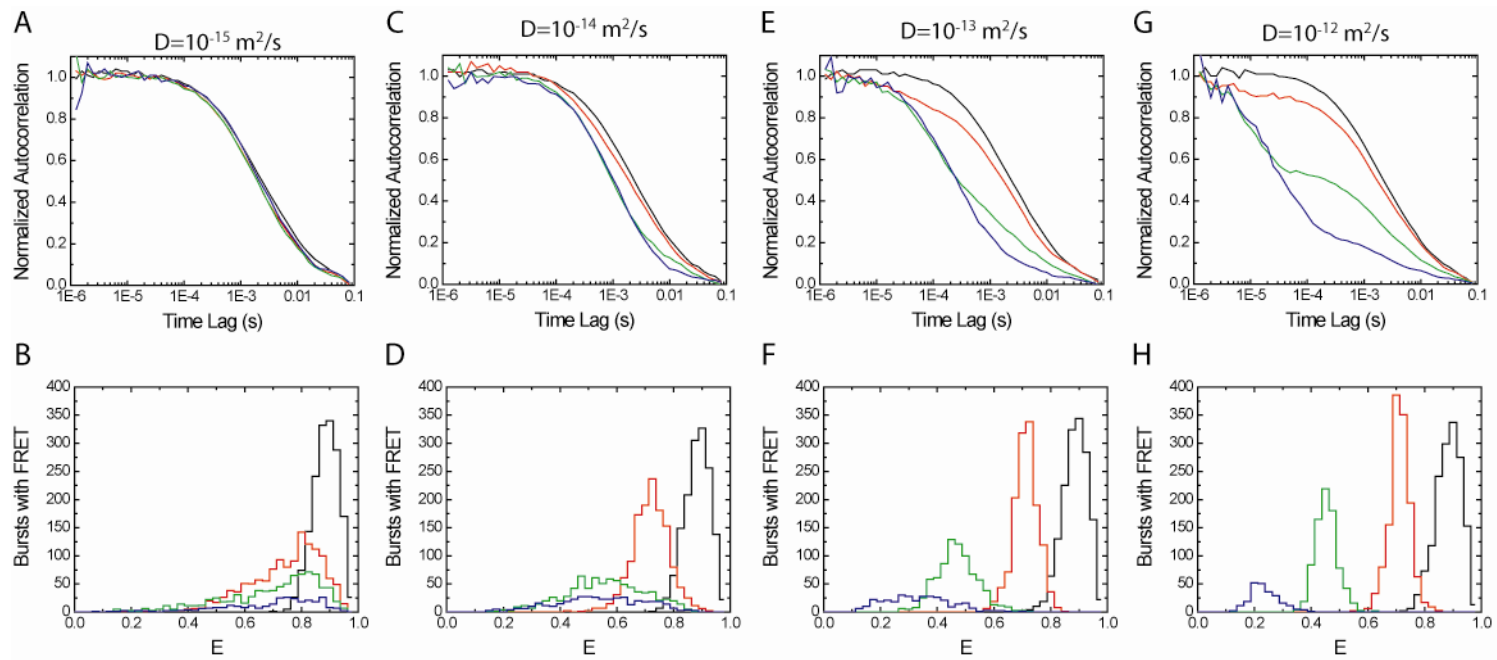
Figure 4
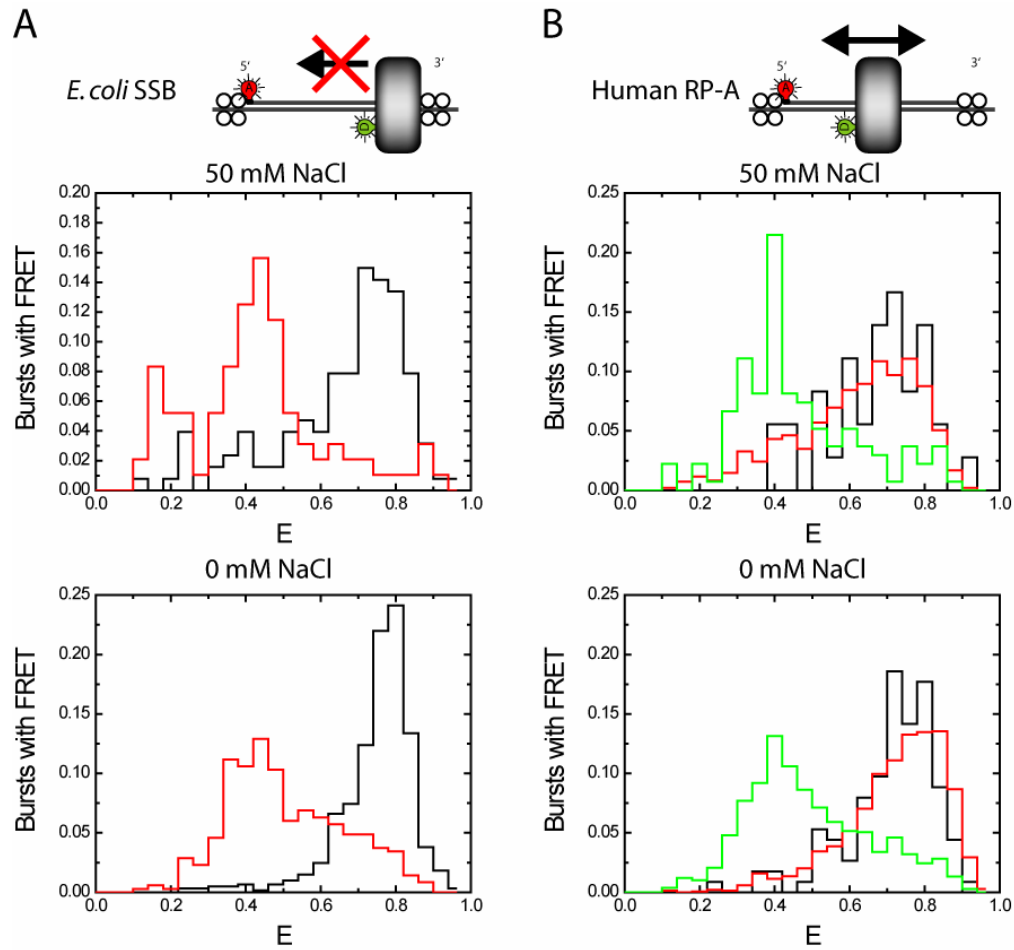
Figure 5
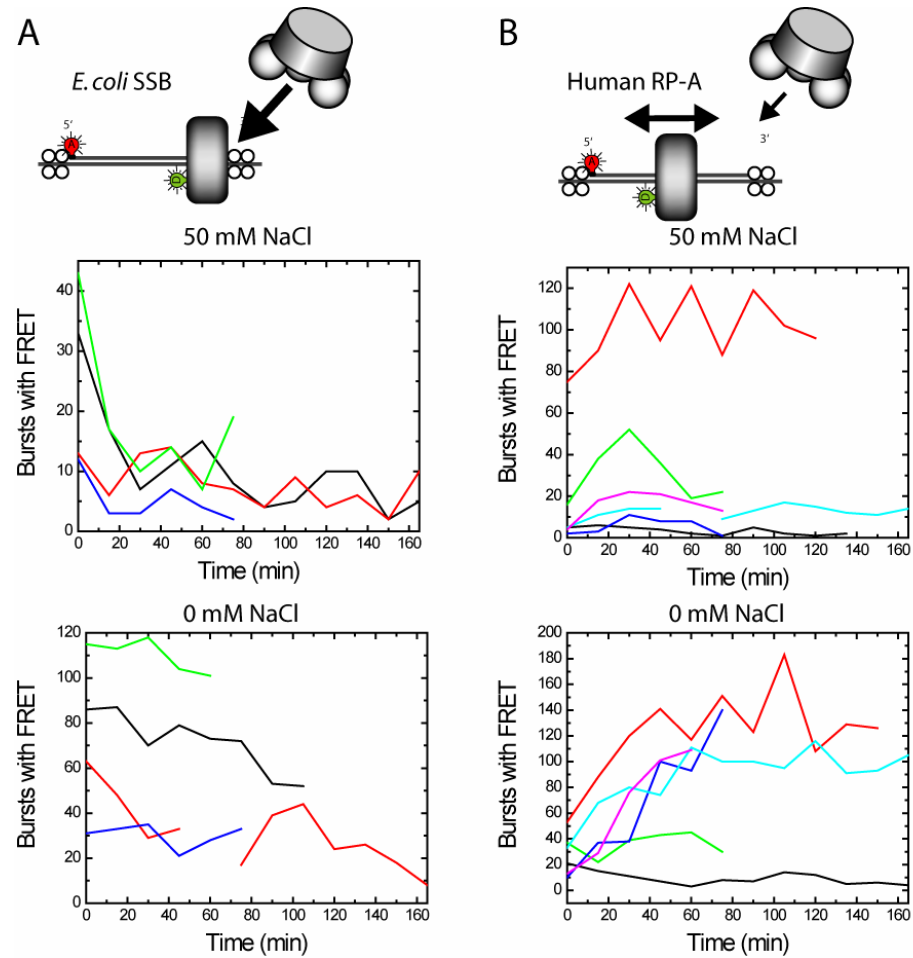
Figure 6
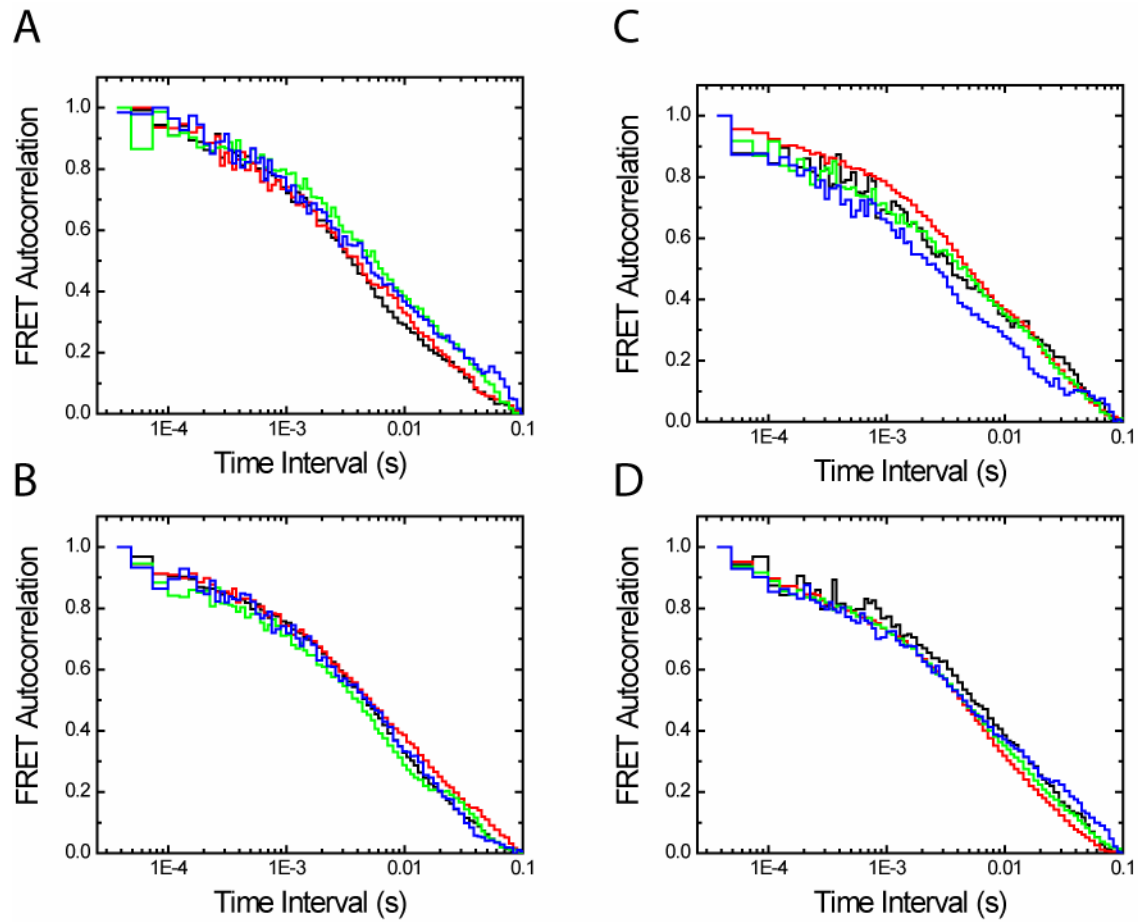
Figure 7
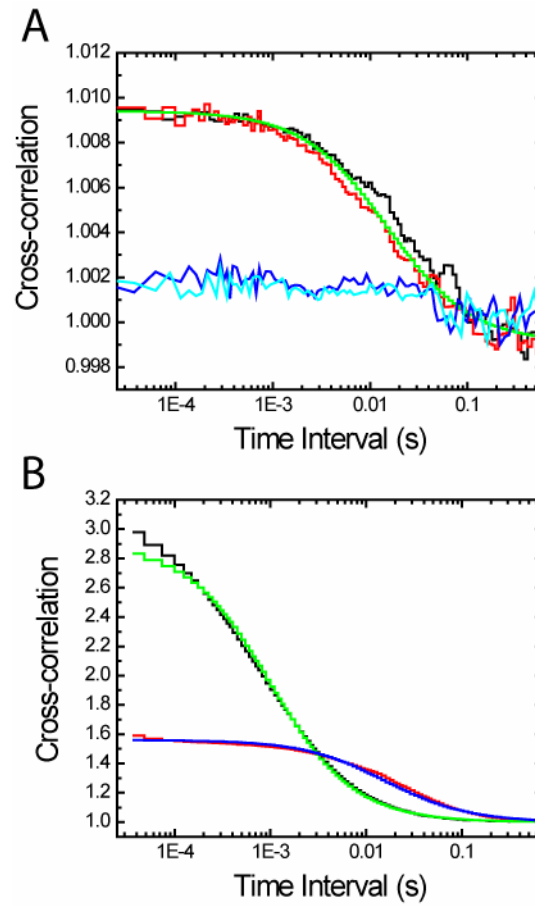
Table 1

Accessory Protein	Added NaCl	18	30	45	90
SSB	50 mM	-2E-4 ± 6E-4	9E-4 ± 6E-4	3E-3 ± 1E-3	2E-3 ± 1E-3
	0 mM	3E-3 ± 1E-3	4E-3 ± 1E-3	6E-3 ± 1E-3	6E-3 ± 2E-3
RP-A	50 mM	2E-3 ± 1E-3	4E-3 ± 2E-3	5E-3 ± 2E-3	1.0E-2 ± 1E-3
	0 mM	4E-3 ± 2E-3	4E-3 ± 1E-3	1E-2 ± 1E-3	2.1E-2 ± 2E-3
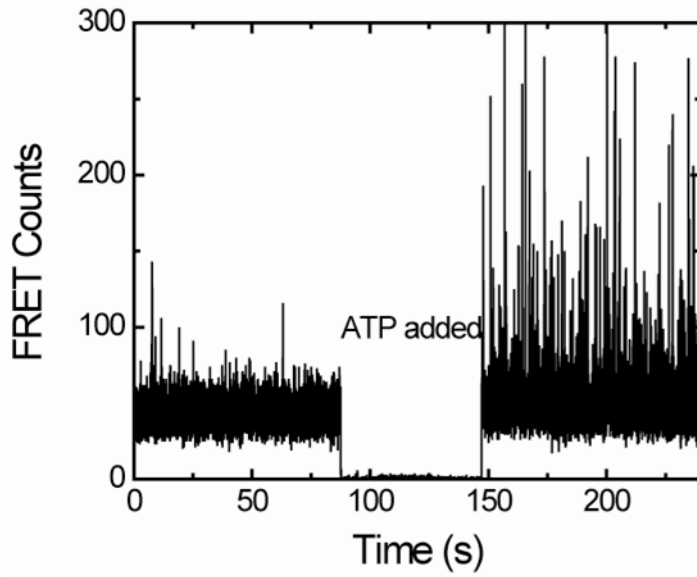
Figure S1: Complexes of β clamp with DNA undergoing FRET are visible only upon adding ATP to a solution also containing the clamp loader complex. Each spike in the time trace is due to the transit of a single β clamp-DNA complex undergoing FRET through the detection volume. In the experiment shown, ATP was added to the reaction mixture after two minutes. As indicated by simultaneous, bright bursts in the D channel (not shown), the infrequent bursts seen in the FRET channel are due to leakage of D signal from aggregates of β clamp. The FRET events seen after adding ATP are accompanied by simultaneous bursts seen by directly exciting the acceptor.
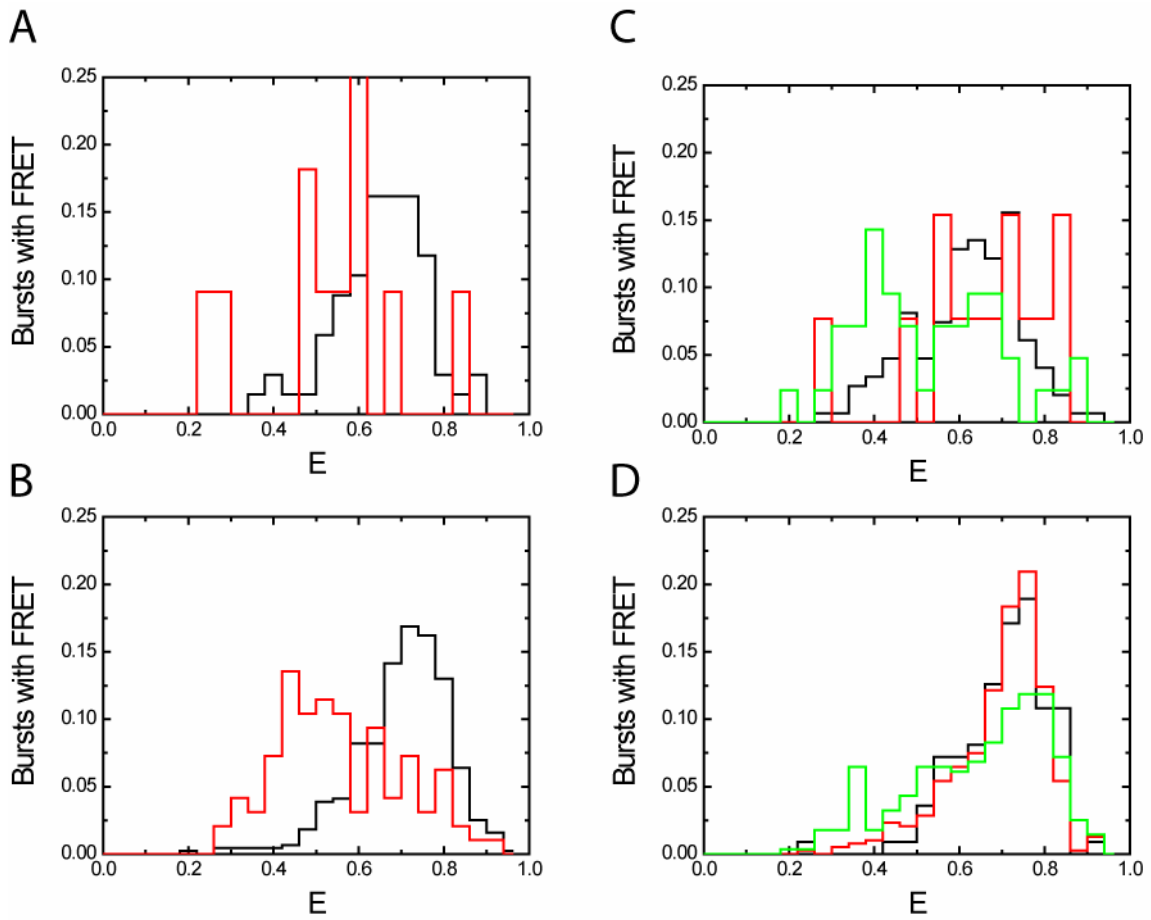
Figure S2: Same as Figure 5, but the DNA oligomers are annealed to site 2 on the DNA plasmid. The experiments are 90 minutes in length, rather than 180 minutes.
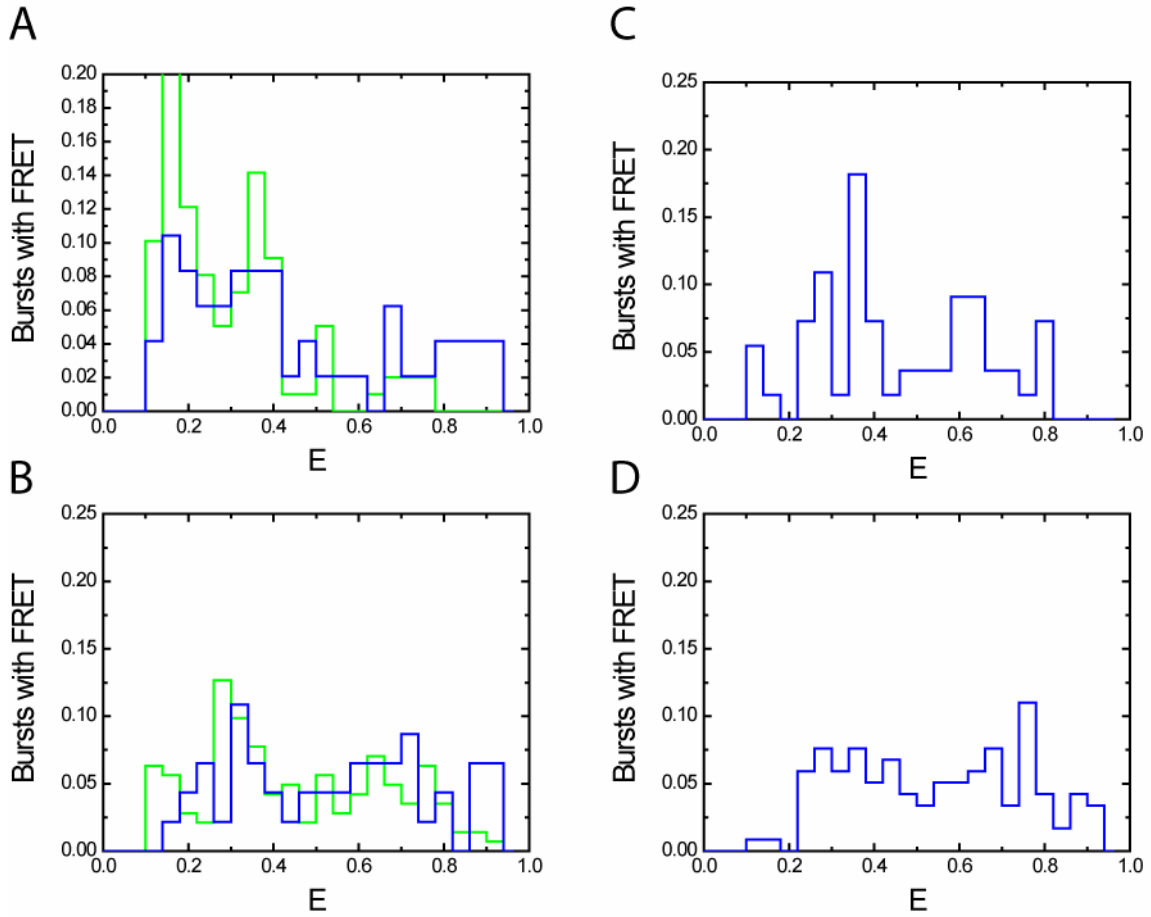
Figure S3: The histograms for the 45mer and 90mer annealed to site 1 of the DNA plasmid not shown in Figure 5. The 45mer data is shown in green, whereas the 90mer data is shown in blue.
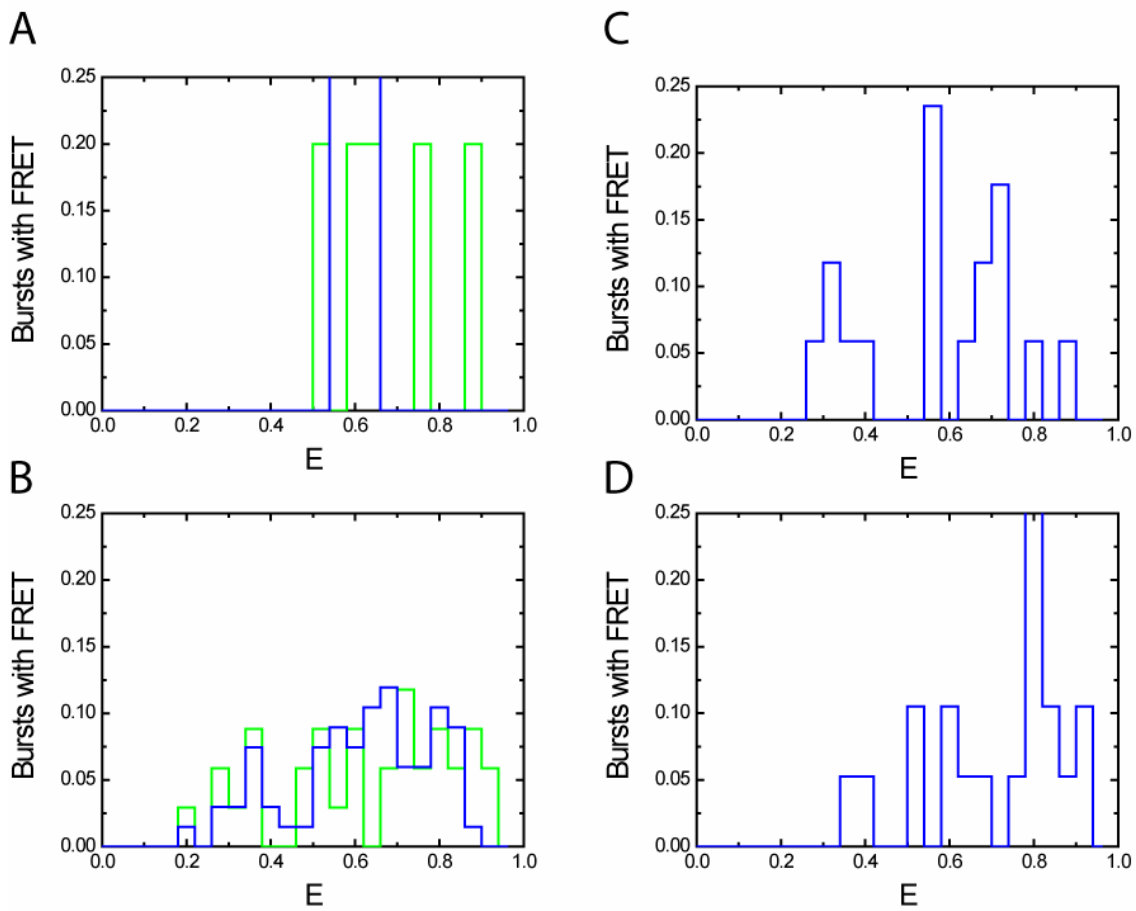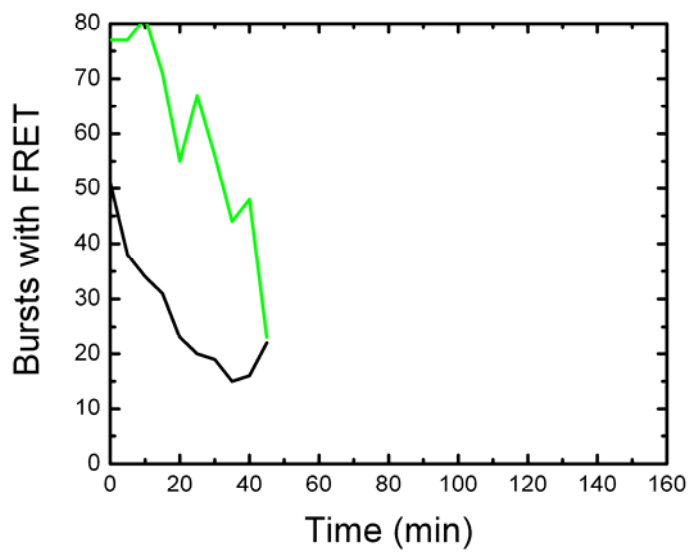
Figure S4: The histograms for the 45mer and 90mer annealed to site 2 of the DNA plasmid not shown in Figure S1. The 45mer data is shown in green, whereas the 90mer data is shown in blue.

Figure S5: Kinetic data of loading/unloading monitored as shown in Figure 6 for clamp overloading experiments. If ATP consumption were the cause of the decrease in number of FRET events seen here and in Figure 6, the decrease should be much faster here, with 25X the concentration of clamp and clamp loader (?), and 1/3 the concentration of DNA plasmid. For site 1 on the DNA plasmid, the 18mer is shown in black. For site 2, the 18mer is shown in green.
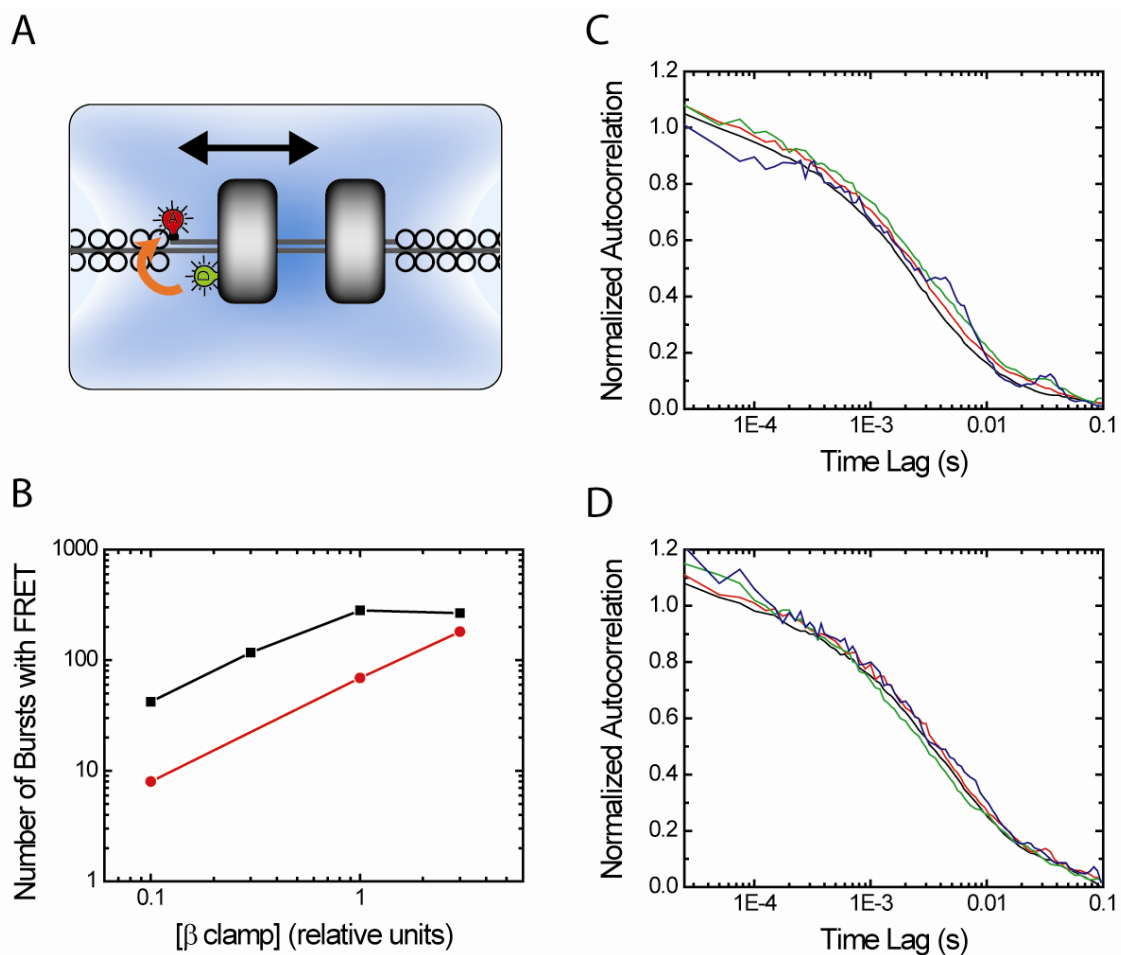
Figure S6: Clamp overloading experiments do not reveal movement of the sliding clamp on DNA within our observation time. A. For longer DNA oligomers (30mer, 45mer, and 90mer), loading with additional β clamps may allow free movement of the clamp for observation of diffusion on DNA. B. The conditions chosen were saturating for the 18mer (black line), but not high enough to saturate the 90mer (red line). Presumably, this will allow free movement of additional clamps (barring significant clamp-clamp interactions). C. PFCS autocorrelations of the FRET signal extracted for the fluorescence bursts showing significant FRET counts. No evidence for FRET movement is seen. DNA primers were attached to site 1 of the DNA plasmid. D. Same as C, but the DNA primers were attached to site 2 of the DNA plasmid.
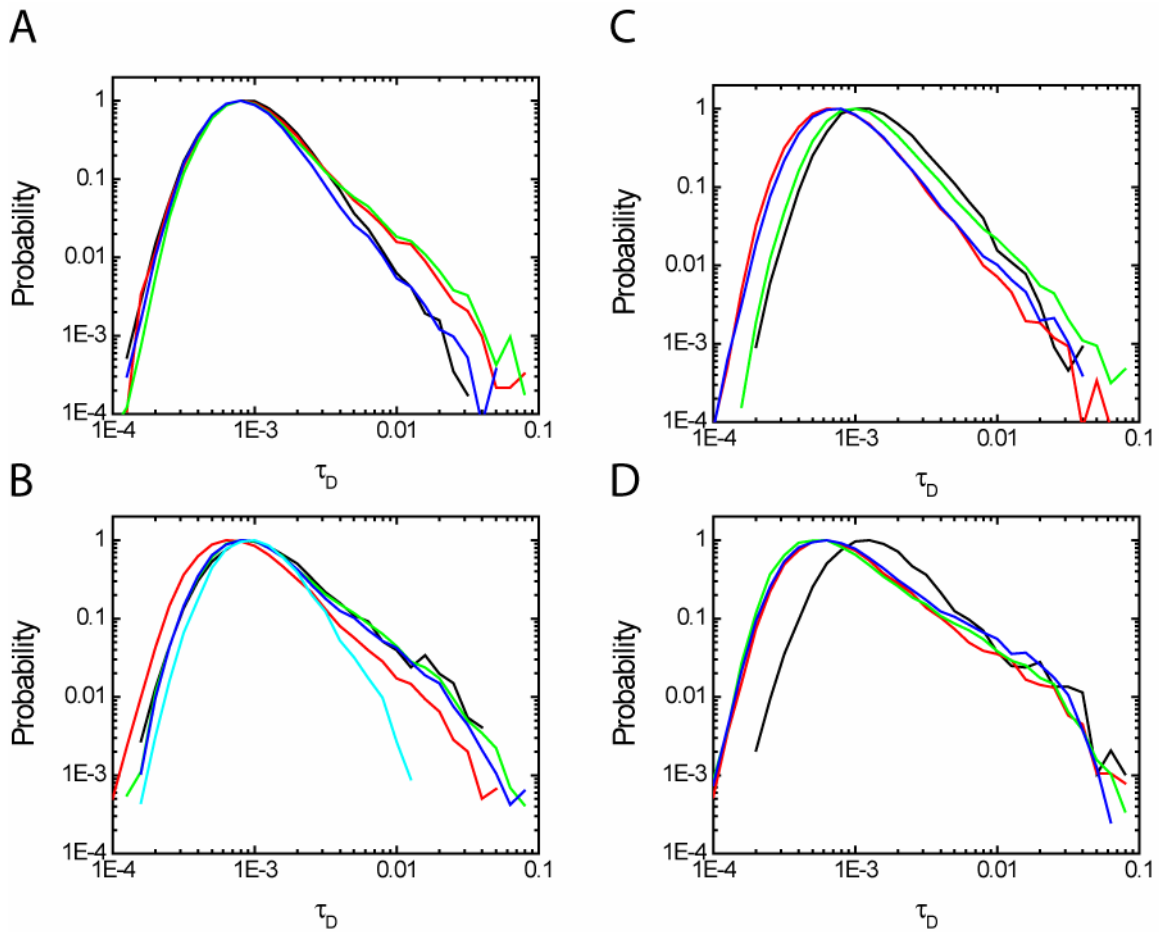
Figure S7: Histograms of diffusion times τ_D fitted for single molecule fluorescence bursts in the donor channel. The bursts were expanded by 100 ms on both sides of the burst before calculating the autocorrelation and fitting to extract the diffusion time. The shoulders in the histograms toward long τ_D correspond to the larger β clamp-DNA complexes. Black: 18mer; red: 30mer; green: 45mer; blue: 90mer. The cyan is for the 18mer without ATP; the much-reduced shoulder indicates the lack of loading of β clamp onto DNA. Conditions are as follows. A. SSB, 50 mM NaCl. B. SSB, 0 mM NaCl. C. RP-A, 50 mM NaCl. D. RP-A, 0 mM NaCl.
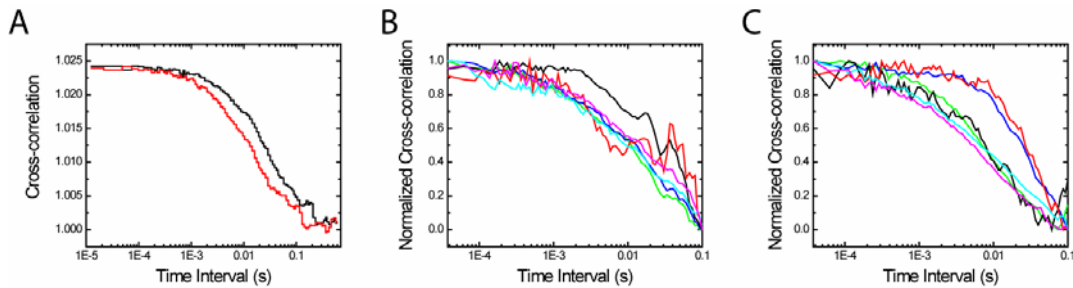
Figure S8: Asymmetry in cross-correlations reveals photobleaching. Black: "donor preceding acceptor" cross-correlation. Red: "acceptor preceding donor" cross-correlation. Green: "donor preceding FRET" cross-correlation. Blue: "FRET preceding donor" cross-correlation. Cyan: "FRET preceding acceptor" cross-correlation. Magenta: "acceptor preceding FRET" cross-correlation. A. Cross-correlations over entire experiments similar to those shown in Figure 7A, except this experiment is using RP-A with 0 mM NaCl. The "donor preceding acceptor" cross-correlation has a longer correlation decay time than the "acceptor preceding donor" correlation, indicating that the donor photobleaches before the acceptor. B. Using PFCS to select only those bursts showing FRET, similar cross-correlations for the donor-acceptor cross-correlations are found (although more noisy). C. PFCS cross-correlations are shown for the experiments with 18mer at site 1, SSB, and 0 mM NaCl. In these experiments, a large number of bursts with FRET were observed. In this case, the "acceptor preceding donor" and "FRET preceding donor" cross-correlations were significantly longer than their counterparts. This indicates that, in the bursts with significant FRET, the acceptor was photobleaching before the donor.
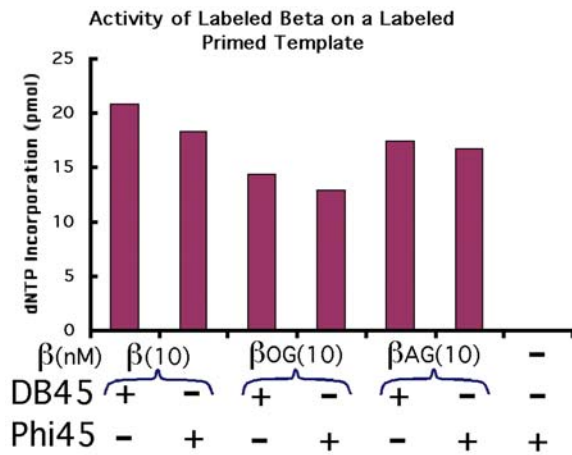
Figure S9: The labeling of the β clamp with Alexa 488 does not significantly affect activity of the β clamp. The effect may be larger than shown in the graph, since 80% of the clamps are unlabeled. Since the β clamp forms a dimer, 64% of the dimers will have no label. If the labeled β clamp were not active, the incorporated dNTP should be reduced by 30%.